Inorganic Chemistry

Article

pubs.acs.org/IC

Synthesis, Crystal and Electronic Structures of the New Zintl phases $Ba_3Al_3Pn_5$ (*Pn* = P, As) and $Ba_3Ga_3P_5$

Hua He, Chauntae Tyson, Maia Saito, and Svilen Bobev*

Department of Chemistry and Biochemistry, University of Delaware, Newark, Delaware 19716, United States

Supporting Information

ABSTRACT: The new Zintl compounds $Ba_3Al_3P_5$, $Ba_3Al_3As_5$, and $Ba_3Ga_3P_5$ have been synthesized using molten metal fluxes. They are isoelectronic and isotypic, crystallizing with a novel rhombohedral structure type in the space group $R\bar{3}c$ with unit cell constants a = 14.5886(9) Å, c = 28.990(3) Å for $Ba_3Al_3P_5$, a = 14.613(3) Å, c = 28.884(8) Å for $Ba_3Ga_3P_5$, and a = 14.9727(13) Å, c = 29.689(4) Å for $Ba_3Al_3As_5$, respectively. The structures are based on $TrPn_4$ (*Tr* = Al, Ga; *Pn* = P, As) tetrahedra that share both edges and corners, leading to intricate arrangements embodied in the $[Tr_4Pn_9]^{15-}$ and $[Tr_3Pn_6]^{9-}$ strands, interconnected by dimeric $[Tr_2Pn_6]^{12-}$ units. The Ba^{2+} cations reside within cylindrical channels within the polyanionic framework and provide the valence electrons needed for *Tr*–*Pn* covalent bonding. In spite of the large and complex structure, there are no homoatomic *Tr*–*Tr* or *Pn*–*Pn* interactions, hence, the structures can be readily rationalized in the context of the Zintl–Klemm formalism as follows $[Ba^{2+}]_3[Tr^{3+}]_3[Pn^{3-}]_5$; calculations on their electronic band-structures confirm this reasoning and reveal about 1.4–1.9 eV energy band gaps, that is, semiconducting behavior. Structural parallels with other known Zintl compounds are also presented.

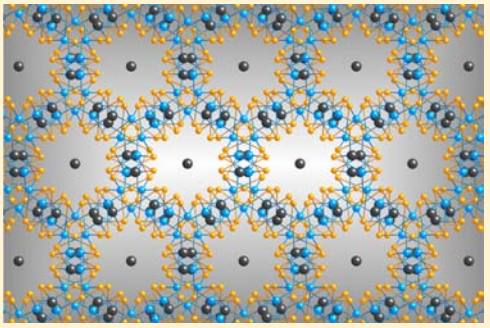

INTRODUCTION

In the past 5–6 years, we have actively been involved in research on *AE*-*Tr*-*Pn* ternary pnictides, where *AE* = Ca, Sr, Ba, Eu, Yb; *Tr* = Al, Ga, In; and *Pn* = P, As, Sb.[1−7] Despite the fact that exploratory studies in the 1980s have turned up a large number of compounds in these systems,[8] based on our work and on recent reports by other groups working in this area, one can speculate of the numerous opportunities for new material discoveries, which remain therein. Some specific examples which attest for the rich "phase-space" include $BaGa_2Sb_2$,[9] $Yb_5Al_2Sb_6$,[10] $Ba_2In_5As_5$,[11] Eu_3InP_3,[12] $Eu_3In_2P_4$,[13] $EuIn_2P_2$,[14] $EuGa_2As_2$,[15] $Ba_3Ga_4Sb_5$,[16] and $Eu_7Ga_6Sb_8$,[17] among others. Notably, almost without exceptions, the compounds above could be classified as Zintl phases,[18,19] in which the more electropositive elements (*AE*) are electron donors, while the more electronegative elements (*Tr* and *Pn*) accept these electrons to fill their valence electron shells and to form covalent bonds. Thus, in such compounds, the electron balance resembles the classic semiconductors, an analogy that can also be justified by the energy band gaps usually present in their electronic structures.[20] These structural and bonding characteristics make the Zintl phases promising candidates for thermoelectric applications,[21−23] and indeed, several high-*ZT* efficiency compounds have already been identified,[24−29] with Ca_3AlSb_3[28] and $Ca_5Al_2Sb_5$[29] being among the most recent ones.

Our prior work on pnictides has shown remarkable structural diversity, as exemplified by the series of $AEGa_2As_2$ (*AE* = Ca, Sr, Ba) and $CaGa_2P_2$, each crystallizing with its own structure.[5,6] Notably, all of them were synthesized in high yields from molten fluxes, while the conventional high temperature routes produced multicomponent mixtures. Taking advantage of the flux method, which has been proved to be an effective way toward new compounds,[30] we continued the exploratory work and identified the novel compounds $Ba_3Ga_3P_5$ and $Ba_3Al_3Pn_5$ (*Pn* = P, As). With this paper, we report the results from this synthetic/structural work, alongside a discussion of the chemical bonding in this complex rhombohedral structure.

EXPERIMENTAL SECTION

Synthesis. All manipulations of the starting materials and the reaction products were conducted inside an Ar-filled glovebox or under vacuum. The elements (the alkaline-earth metals, Al, Ga, As, and Pb) were purchased from either Alfa-Aesar or Aldrich with the stated purity greater than 99.9% (metal basis), and were used as received. Red phosphorus powder had a stated purity 99%. Crystals of $Ba_3Ga_3P_5$ were initially identified from a reaction of the elements Ba, Ga, P, and Pb with a 2:1:2:20 molar ratio. The mixture was contained in an alumina crucible, where the excess amount of Pb was intended as a flux to facilitate the crystal growth. The crucible was then jacketed in a fused-silica tube, which was subsequently flame-sealed under vacuum. Heat treatment included a ramp to 960 °C over 14 h, a "soak" at that temperature for 40 h, followed by cooling to 500 °C during a period of 16 h. Then, the reaction was taken out of the furnace, and the Pb flux was removed. The small, air-sensitive crystals, which appeared to be dark-red when cut under a microscope turned out to be $Ba_3Ga_3P_5$, following structure determination by single-crystal X-ray diffraction. Another product of the same reaction were black, pebble-like crystals of $Ba_7Ga_4P_9$.[31] Similar reaction with arsenic did not

Received: November 7, 2012
Published: December 18, 2012

   dx.doi.org/10.1021/ic302437t | *Inorg. Chem.* 2013, 52, 499–505

produce $Ba_3Ga_3As_5$; only $Ba_7Ga_4As_9$ was identified from the corresponding reaction.[31] Analogous reactions with Ca and Sr produced only $Ca_3Ga_2P_4$ and $Sr_3Ga_2Pn_4$ (Pn = P, As) with the $Ca_3Al_2As_4$ type[7] and $Ca_{14}GaAs_{11}$ with the $Ca_{14}MnAs_{11}$ type.[32]

After the structure and composition of $Ba_3Ga_3P_5$ were established, new reactions with the correct Ba:Ga:P stoichiometry and Pb in 30-fold excess were carried out, but they failed to produce the desired phase; the major product was $Ba_4Ga_5P_8$.[6] As seen from Figure 1, the

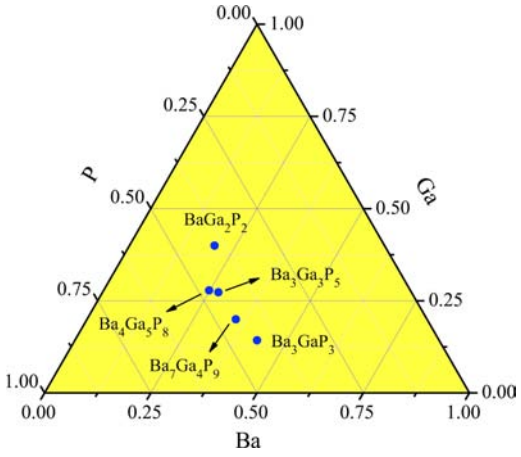

Figure 1. Known ternary compounds in the Ba−Ga−P phase diagram.

composition of $Ba_3Ga_3P_5$ is very close to that of $Ba_4Ga_5P_8$, which might explain the observed reaction outcomes. Using this diagram for guidance, we can speculate that under the given reaction conditions, when Ba is in excess, the formation of $Ba_3Ga_3P_5$ would be favored; however, this would also lead to the inevitable formation of $Ba_7Ga_4P_9$. Reactions using Ga as a self-flux were tried, too, but produced only a mixture of $BaGa_2P_2$,[5] $BaGa_4$,[33] and GaP.[33] One possible explanation is that under the studied conditions, Ba reacts quickly with the flux metal and readily forms other crystalline products, particularly the highly stable phase $BaGa_4$.[33] Therefore, the use of Pb flux appears to be a better synthetic route toward $Ba_3Ga_3P_5$.

Stoichiometric reactions (without the flux) were also carried out by heating a 3:3:5 mixture of Ba, Ga, and P in alumina crucibles, sealed in evacuated fused silica tube. The reaction was conducted at 900 °C for 24 h, followed by an annealing at 500 °C for 1 week. The two main products of such reaction were $Ba_7Ga_4P_9$ and $Ba_3Ga_3P_5$. The presence of $Ba_7Ga_4P_9$ is suggestive of this phase being the thermodynamically stable product at these conditions and running the above reaction at 900 °C for 24 h, followed by cooling to room temperature confirms this thinking—the reaction produced only one ternary phase—$Ba_7Ga_4P_9$, plus traces of GaP and leftover Ga.

Following the work in the Ba−Ga−P/Ba−Ga−As systems, we then moved to the corresponding Ba−Al−P/Ba−Al−As systems. Reactions using excess Al as a fluxing agent afforded $Ba_3Al_3P_5$ and $Ba_3Al_3As_5$, both being air-sensitive. In these reactions, Ba, Al, and P (or As) were loaded with the 1:20:2 ratio and were heated at 960 °C for 20 h, and then cooled at a rate of 10 °C/h to 750 °C, at which temperature the excess Al flux was removed. Caution had to be taken because of the high reactivity of the molten Al with silica. Except for $Ba_3Al_3P_5$ and $Ba_3Al_3As_5$, $Ba_3Al_2P_4$ and $Ba_3Al_2As_4$ were also identified from these reactions.[7] Growing $Ba_3Al_3P_5$ and $Ba_3Al_3As_5$ crystals from Pb flux was also attempted, but the products were multiphase mixtures of $Ba_3Al_2Pn_4$, Ba_3As_4, Ba_5P_9, and $AlPn$.[33] Synthetic efforts were also extended to the lighter alkaline-earth metals Ca and Sr employing different fluxes and heat treatments, but none of these reactions produced the targeted phases.

X-ray Powder Diffraction. X-ray powder diffraction data were taken at room temperature on a Rigaku MiniFlex powder diffractometer with Cu Kα radiation. The obtained patterns were very convoluted because of the complex structure and the frequent presence of secondary phases. An additional complication on the analysis of the powder patterns was the fact that all three title compounds are air-sensitive and decompose quickly upon exposure to air.

Single Crystal X-ray Diffraction. X-ray single-crystal diffraction data were collected on a Bruker SMART CCD-based diffractometer, employing monochromated Mo Kα radiation. Crystals from freshly prepared samples were cut under oil to suitable sizes (<100 μm), and were then mounted on glass fibers and quickly transferred onto the goniometer. A cold nitrogen stream (200(2) K) was used to harden the oil and to protect the crystals from being oxidized during the data collection. After ensuring crystal quality by rapid scans, full spheres of data were collected in four batch runs with frame width of 0.3° for ω and θ. Data collection and data integration were done using SMART[34] and SAINTplus[35] programs, respectively. SADABS[36] was used for semiempirical absorption correction based on equivalent reflections. The structures were solved by direct methods and refined by full matrix least-squares on F^2 using SHELXL.[37] In the last refinement cycles, the unit cell axes and the atomic coordinates were standardized with the aid of the Structure TIDY program.[38] Crystal data and refinement parameters are summarized in Table 1; positional and equivalent isotropic displacement parameters and the selected bond distances and angles are listed in Tables 2 and 3, respectively. The crystallographic information file (CIF) has also been deposited with Fachinformationszentrum Karlsruhe, 76344 Eggenstein, Leopoldsha-

Table 1. Crystallographic Data and Refinement Parameters of $Ba_3Ga_3P_5$, $Ba_3Al_3P_5$, and $Ba_3Al_3As_5$

empirical formula	$Ba_3Ga_3P_5$	$Ba_3Al_3P_5$	$Ba_3Al_3As_5$
fw, g mol^{-1}	776.03	647.81	867.56
crystal system		rhombohedral	
space group		$R\bar{3}c$ (No. 167), Z = 18	
λ, Å		0.71073	
T, K		200(2)	
a, Å	14.613(3)	14.5886(9)	14.9727(13)
c, Å	28.884(8)	28.990(3)	29.689(4)
V, Å^3	5341(2)	5343.2(7)	5764.0(10)
ρ_{calcd}, g cm^{-3}	4.343	3.624	4.499
μ (Mo Kα), cm^{-1}	171.20	106.75	220.90
GOF on F^2	1.037	1.078	1.038
R_1 [$I > 2\sigma(I)$][a]	0.0273	0.0181	0.0217
wR_2 [$I > 2\sigma(I)$][a]	0.0467	0.0407	0.0382
R_1 [all data][a]	0.0400	0.0223	0.0292
wR_2 [all data][a]	0.0505	0.0425	0.0403

[a] $R_1 = \sum||F_o| - |F_c||/\sum|F_o|$; $wR_2 = [\sum[w(F_o^2 - F_c^2)^2]/\sum[w(F_o^2)^2]]^{1/2}$, and $w = 1/[\sigma^2F_o^2 + (A\cdot P)^2 + B\cdot P]$, $P = (F_o^2 + 2F_c^2)/3$; A and B are weight coefficients as follows: A = 0.0153 and B = 25.5 for $Ba_3Ga_3P_5$, A = 0.0212 and B = 10.15 for $Ba_3Al_3P_5$, A = 0.0116 and B = 0 for $Ba_3Al_3As_5$.

Table 2. Atomic Coordinates and Equivalent Isotropic Displacement Parameters (U_{eq}[a]) for $Ba_3Ga_3P_5$

atom	Wyckoff Site	x	y	z	U_{eq} (Å^2)
Ba1	36f	0.1977(1)	0.3101(1)	0.1612(1)	0.013(1)
Ba2	12c	0	0	0.1012(1)	0.016(1)
Ba3	6a	0	0	1/4	0.011(1)
Ga1	36f	0.2987(1)	0.1061(1)	0.1176(1)	0.011(1)
Ga2	18e	0.2705(1)	0	1/4	0.012(1)
P1	36f	0.2011(1)	0.0656(1)	0.1887(1)	0.011(1)
P2	36f	0.2253(1)	0.1841(1)	0.0695(1)	0.012(1)
P3	18e	0.6255(2)	0	1/4	0.013(1)

[a] U_{eq} is defined as one-third of the trace of the orthogonalized U^{ij} tensor

dx.doi.org/10.1021/ic302437t | Inorg. Chem. 2013, 52, 499−505

Table 3. Important Interatomic Distances (Å) in $Ba_3Ga_3P_5$, $Ba_3Al_3P_5$, and $Ba_3Al_3As_5$

$Ba_3Ga_3P_5$		$Ba_3Al_3P_5$		$Ba_3Al_3As_5$	
Ga1−P1	2.399(2)	Al1−P1	2.401(1)	Al1−As1	2.485(2)
Ga1−P1	2.524(2)	Al1−P1	2.474(1)	Al1−As1	2.569(2)
Ga1−P2	2.367(2)	Al1−P2	2.346(1)	Al1−As2	2.437(2)
Ga1−P3	2.328(1)	Al1−P3	2.320(1)	Al1−As3	2.405(2)
Ga2−P1 (2×)	2.460(2)	Al2−P1 (2×)	2.446(1)	Al2−As1 (2×)	2.540(1)
Ga2−P2 (2×)	2.388(2)	Al2−P2 (2×)	2.364(1)	Al2−As2 (2×)	2.457(1)
P1−Ga1	2.399(2)	P1−Al1	2.401(1)	As1−Al1	2.485(2)
P1−Ga1	2.524(2)	P1−Al1	2.474(1)	As1−Al1	2.569(2)
P1−Ga2	2.460(2)	P1−Al2	2.446(1)	As1−Al2	2.540(1)
P2−Ga1	2.367(2)	P2−Al1	2.346(1)	As2−Al1	2.437(1)
P2−Ga2	2.388(2)	P2−Al2	2.364(1)	As2−Al2	2.457(1)
P3−Ga1 (2×)	2.328(1)	P3−Al1 (2×)	2.320(1)	As3−Al1 (2×)	2.405(1)
Ba1−P1	3.482(2)	Ba1−P1	3.4147(9)	Ba1−As1	3.5093(6)
Ba1−P2	3.153(2)	Ba1−P2	3.1495(8)	Ba1−As2	3.2196(6)
Ba1−P2	3.199(2)	Ba1−P2	3.1994(8)	Ba1−As2	3.2881(6)
Ba1−P2	3.363(2)	Ba1−P2	3.3489(8)	Ba1−As2	3.4483(6)
Ba1−P3	3.344(2)	Ba1−P3	3.3614(9)	Ba1−As3	3.4370(6)
Ba1−P3	3.421(1)	Ba1−P3	3.4364(6)	Ba1−As3	3.5215(5)
Ba2−P1 (3×)	3.623(2)	Ba2−P1 (3×)	3.6315(9)	Ba2−As1 (3×)	3.6700(7)
Ba2−P2 (3×)	3.171(2)	Ba2−P2 (3×)	3.1808(8)	Ba2−As2 (3×)	3.2496(6)
Ba3−P1 (6×)	3.142(2)	Ba3−P1 (6×)	3.1543(8)	Ba3−As1 (6×)	3.2056(5)

fen, Germany; fax: (49) 7247-808-666; email: crysdata@fiz.karls-ruhe.de; depository numbers CSD-425290 ($Ba_3Al_3P_5$), CSD-425291 ($Ba_3Ga_3P_5$), CSD-425292 ($Ba_3Al_3As_5$).

Electronic Structure Calculation. The Stuttgart TB-LMTO 4.7 program[39] was used to calculate electronic band structures. Local density approximation (LDA) was used to treat exchange and correlation.[40] All relativistic effects except for spin−orbital coupling were taken into account by the scalar relativistic approximation.[41] The basis set included the 5d, 6s, and 6p orbitals for Ba, 4s, 4p, and 4d orbitals for Ga, 3s, 3p, and 3d orbitals for Al, 4s, 4p, and 4d orbitals for As, and 3s, 3p, and 3d orbitals for P. The *k*-space integrations were performed by the tetrahedron method,[42] using 65 irreducible *k*-points in the Brillouin zone. The total and partial density of states (DOS) were computed and studied. To interrogate the chemical bonding, crystal orbital Hamiltonian populations (COHP)[43] of selected interactions were also analyzed.

RESULTS AND DISCUSSION

Structure. All three compounds are isoelectronic and isostructural, crystallizing in the rhombohedral space group $R\bar{3}c$ (No. 167, Pearson symbol *hR*198). This appears to be a new structure type since a search in the Pearson's Handbook,[33] and the latest edition of the Inorganic Crystals Structure Database (ICSD)[44] did not reveal any known phases with the same space group and Wyckoff letters. The structure contains eight crystallographically independent atoms—three Ba, two Ga or Al, and three pnictogen atoms (Table 2). For the sake of conciseness, the detailed discussion of the structure will focus on $Ba_3Ga_3P_5$ only.

In the context of the Zintl−Klemm formalism,[18−20] the structure of $Ba_3Ga_3P_5$ constitutes Ba^{2+} cations and $[Ga_3P_5]^{6-}$ polyanions based on GaP_4 tetrahedra. The polyanionic 3-dimensional network is based on a complex pattern of corner- and edge-shared GaP_4 tetrahedra. Projected down the *c* axis (Figure 2), cylindrical channels formed by the polyanionic strands can be seen; Ba2 and Ba3 atoms are residing within these channels, whereas Ba1 atoms are "hidden" among the strands. The "knotty" polyanionic substructure is easier to be understood if the unit cell is projected along the [211] direction as shown in Figure 3a. In this view, the substructure

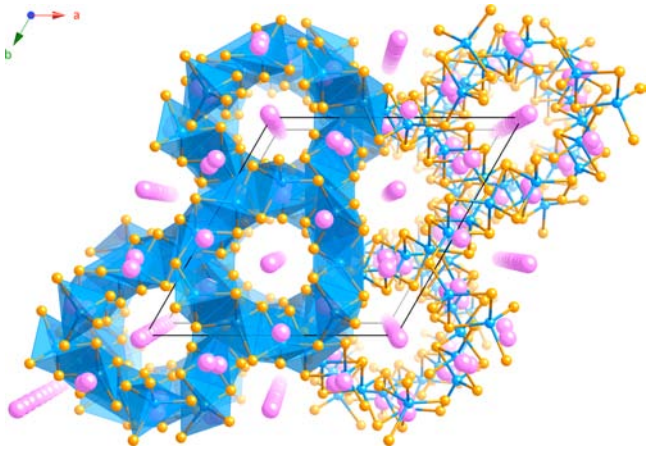

Figure 2. Crystal structure of $Ba_3Ga_3P_5$ projected along the *c* axis, where the GaP_4 tetrahedra are emphasized. Color code: Ba, pink; Ga, blue; P, yellow.

could be considered as being composed of smaller components: $[Ga_4P_9]^{15-}$ and $[Ga_3P_6]^{9-}$ ribbons, and $[Ga_2P_6]^{12-}$ dimers of edge-shared tetrahedra as bridging units. Figure 3b and Figure 3c show "unfolded" $[Ga_4P_9]^{15-}$ and $[Ga_3P_6]^{9-}$ fragments in the direction they propagate. From the latter views, one will notice that in $[Ga_4P_9]^{15-}$, four GaP_4 tetrahedra are fused by common edges to form a Ga_4P_{10} motif, which is connected with the neighboring Ga_4P_{10} units by corner-sharing. On the other hand, the $[Ga_3P_6]^{9-}$ strand can be broken to trimeric Ga_3P_8 motifs made of three edge-shared GaP_4 tetrehedra, pivoting around a P atom. The Ga_3P_8 motifs are the "repeating unit" of the $[Ga_3P_6]^{9-}$ strand, where only edge-sharing mode exists. The Ga_2P_6 spacers link the $[Ga_4P_9]^{15-}$ strands by common edges and the $[Ga_3P_6]^{9-}$ strands by common corners. It is obvious that since all of the P atoms in the linkers are shared with the strands, the connectors could be thought as contributing only Ga atoms. Therefore, the overall polyanion could be rationalized as follows:

dx.doi.org/10.1021/ic302437t | Inorg. Chem. 2013, 52, 499−505

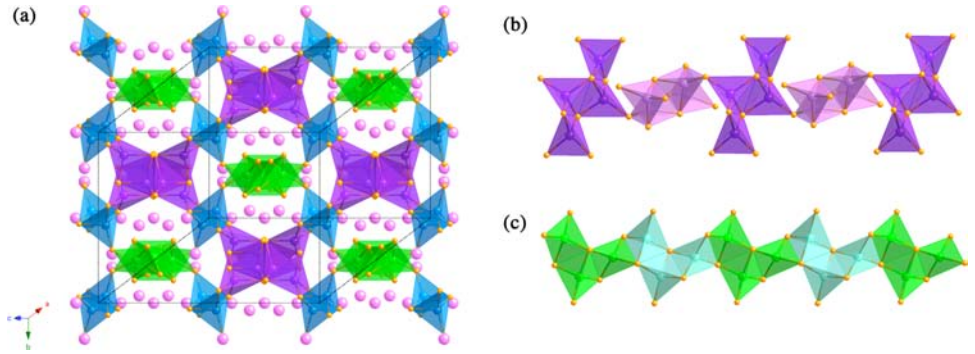

Figure 3. (a) Crystal structure of $Ba_3Ga_3P_5$ projected along the [211] direction, where the purple, green, and blue fragments represent the $[Ga_4P_9]^{15-}$ strands, the $[Ga_3P_6]^{9-}$ strands, and the Ga_2P_6 dimeric tetrahedra linkers for the strands, respectively; (b) the $[Ga_4P_9]^{15-}$ strand and (c) the $[Ga_3P_6]^{9-}$ strand shown as they stretch along the [211] direction.

$$[Ga_4P_9]^{15-} + [Ga_3P_6]^{9-} + 2Ga^{3+} = [Ga_9P_{15}]^{18-} = 3 \times [Ga_3P_5]^{6-}$$

Although $TrPn_4$ tetrahedra are common structural motifs in the triel-pnictides with alkali or alkaline-earth metals, the $^3_\infty[Tr_3Pn_5]^{6-}$ polyanionic network in the title compounds is unique. A search for highly condensed tetrahedral frameworks within these systems (in which the *Tr:Pn* ratio is usually larger than 1:2) reveals several structures, including $K_2Al_2Sb_3$,[45] $K_3Al_2As_3$,[46] $K_3In_2As_3$,[47] $K_3Ga_3As_4$,[48] and $Na_3In_2Bi_3$,[49] among others. However, none of these structures boasts similar polyanionic framework, although some structural parallels can be drawn. For example, In_3As_8 motifs (topologically the same as the Ga_3P_8 motifs shown in Figure 3c), can be noted in the $K_3In_2As_3$ structure.[47] Figure 4 depicts the 2D $[In_2As_3]^{3-}$ polyanionic layers in $K_3In_2As_3$ and how In_3As_8 units are connected by sharing edges with the $InAs_4$ tetrahedral linkers. Another noteworthy observation concerns alkaline-earth metal gallium nitrides with the same stoichiometry—$Sr_3Ga_3N_5$[50] and $Ba_3Ga_3N_5$[51]—which exist, too, but crystallize with different structures. In the structure of $Sr_3Ga_3N_5$, as shown in Figure 5a, the 3D polyanionic $[Ga_3N_5]^{6-}$ framework could be viewed as $[Ga_4N_8]$ slabs formed of tetramers (edge-shared GaN_4), joined via dimeric Ga_2N_6 units (topologically the same as the Ga_2P_6 spacers shown in Figure 3). On the other hand, 1D polyanionic $[Ga_3N_5]^{6-}$ rods are observed in the $Ba_3Ga_3N_5$ structure, where Ga_4N_{10}, Ga_3N_8, and Ga_2N_6 motifs could be easily recognized (Figure 5b). We would like to point out that the diborane-like motif Tr_2Pn_6 is frequently seen in these systems, and also found in structures of $BaGa_2Pn_2$,[5] $Ba_2In_5Pn_5$,[6,11] $Ba_3Ga_4Sb_5$,[16] and so forth.

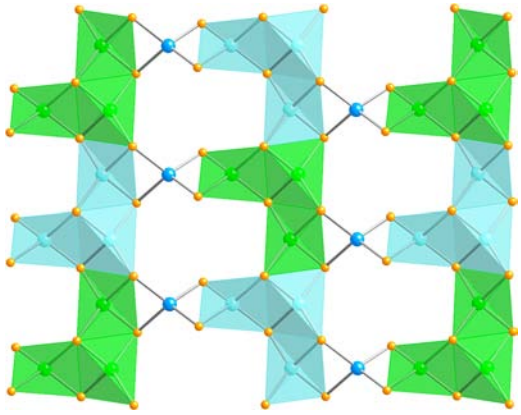

Figure 4. $[In_2As_3]^{3-}$ layer in the $K_3In_2As_3$ structure, where the In_3As_8 motifs are shown in polyhedral presentation. These motifs are fused into $[In_3As_6]$ chains, which are further connected with each other by sharing the edges with the $InAs_4$ tetrahedral linkers.

A brief comment on the interatomic distances is also warranted: the Ga−P bonds measure 2.3277(13)−2.5238(17) Å (Table 3), and compare well with the sum of their Pauling radii (r_{Ga} = 1.246 Å, r_P = 1.10 Å).[52] Ga−P distances in the same range can be found in $BaGa_2P_2$,[5] $CaGa_2P_2$,[6] and Ba_3GaP_3.[53] The Al−P and Al−As distances are also comparable with those in the compounds $AE_3Al_2Pn_4$ (*AE* = Ca, Sr, Ba) and $Eu_3Al_2Pn_4$.[7] We should note, however, that the Al−P distances in $Ba_3Al_3P_5$ are slightly shorter than the Ga−P distances in $Ba_3Ga_3P_5$, which is somewhat surprising since the radius of Al (r_{Al} = 1.248 Å)[52] is very close to that of Ga (in agreement with the unit cell volumes of $Ba_3Ga_3P_5$ and $Ba_3Al_3P_5$). Similar trends can be found by comparing Al−*Pn* bonding in $AE_3Al_2P_4$ and with Ga−*Pn* bonding in $AE_3Ga_2P_4$, respectively. Even the pairs of the III−V semiconductors AlP/GaP and AlAs/GaAs,[33] as well as $Ca_5Al_2Sb_5/Ca_5Ga_2Sb_6$[8] show the same phenomenology, suggesting that this "anomaly" is likely due to the large difference in the electronegativities (Pauling scale: χ_{Al} = 1.5, χ_{Ga} = 1.6, χ_P = 2.1, χ_{As} = 2.0).[52] On the basis of that, one would expect sizable ionic contributions to these very polar Al−*Pn* and Ga−*Pn* interactions, and that the corresponding bond lengths/strengths cannot be directly estimated by using the single-bonded radii from Pauling. We can therefore consider tetrahedrally coordinated Al^{3+}, which is nominally smaller than its Ga-counterpart,[54] to rationalize the understandably shorter Al−*Pn* contacts. While this logic is sound, we argue that treating the Ga−P, Al−P, and Al−As interactions as covalent is a better approach, which is supported by the electronic structure calculations (below). Consequently, we favor the structure description in terms of a $^3_\infty[Tr_3Pn_5]^{6-}$ polyanionic network and Ba^{2+} cations, although the "ionic" formulation $[Ba^{2+}]_3[Tr^{3+}]_3[Pn^{3-}]_5$ remains a valid assumption as well. However, we must note that both attempts to rationalize the structures using simple concepts for bonding cannot be deemed factual, since the LMTO calculations that are discussed next, provide evidence for some degree of covalent interaction between the Ba^{2+} cations and the covalently bounded network.

All Ba atoms are 6-coordinated by P or As atoms, forming distorted $BaPn_6$ octahedra. Such a coordination environment seems common for Ba in ternary pnictides; for example, it is

dx.doi.org/10.1021/ic302437t | *Inorg. Chem.* 2013, 52, 499−505

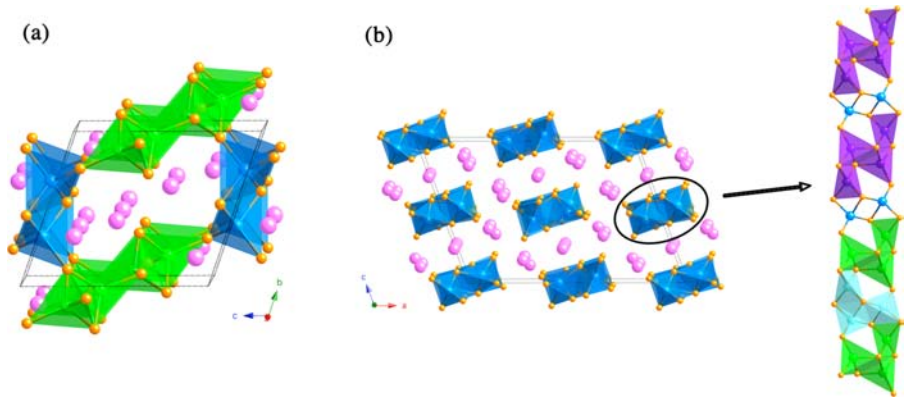

Figure 5. (a) Crystal structure of $Sr_3Ga_3N_5$, where the $[Ga_4N_8]$ strands and the dimeric Ga_2N_6 units are shown in green and blue, respectively. (b) Crystal structure of $Ba_3Ga_3N_5$ (left) and the outstretched vision of one $[Ga_3N_5]$ strand (right), where the structural fragments Ga_4N_{10} and Ga_3N_8 motifs are depicted in purple and green polyhedra, respectively.

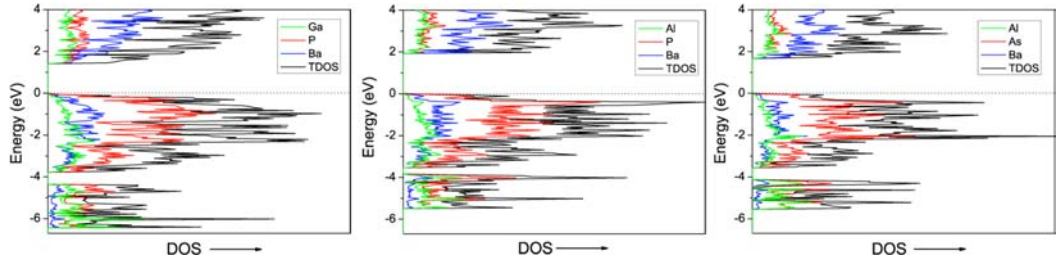

Figure 6. Plots of DOS of $Ba_3Ga_3P_5$, $Ba_3Al_3P_5$, and $Ba_3Al_3As_5$. Total DOS is shown with a solid black line; partial DOS of Ba, Ga/Al, and As/P are represented by blue, green, and red solid lines, respectively. The E_F (dotted line) is the energy reference at 0 eV.

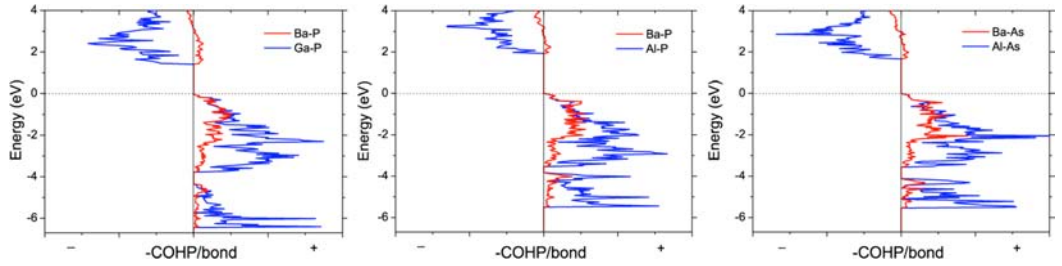

Figure 7. Plots of COHP of $Ba_3Ga_3P_5$, $Ba_3Al_3P_5$, and $Ba_3Al_3As_5$. Contributions from Ba−*Pn* bonding are shown in red, and the Ga−As or Al−*Pn* interactions are shown in blue, respectively. Since the −COHP values are plotted, the "+" regions represent bonding, while the "−" regions denote the antibonding interactions. The E_F (dotted line) is the energy reference at 0 eV.

also seen in $BaGa_2Pn_2$,[5] $Ba_3Al_2Pn_4$,[7] and $Ba_7Ga_2Sb_6$.[3] Comparing the polyhedra around Ba2 and Ba3 (both residing inside the channels—Figure 2) with the polyhedra with Ba1 (residing within the strands), the latter are more distorted, as evidenced from the inequivalent distances between Ba1 and *Pn* (Table 3). Since this structure does not seem to form with the smaller alkaline-earth metals (i.e., Ca and Sr), it can be speculated that efficient space filling cannot be achieved with Ca^{2+} or Sr^{2+}; Ba^{2+} ought to have the "ideal" cation size to fit in the 3D polyanionic framework. This line of thinking could also help explain why $Ba_3In_3As_5$ and any isotypic antimonides could not be synthesized—there are no larger divalent metals than Ba, which can stabilize the very coarse $[In_3As_5]^{6-}$ or $[Ga_3Sb_5]^{6-}$ (hypothetical) frameworks.

Electronic Structure. As mentioned already, there are no *Tr*−*Tr* or *Pn*−*Pn* interactions; therefore, the electron count can be rationalized according to the Zintl−Klemm rules[18−20] as $[Ba^{2+}]_3[Tr^{3+}]_3[Pn^{3-}]_5$. This simplistic description is upheld by the LMTO calculations, which confirm electronic band structures and bonding characteristics as those in the typical semiconductors. The plots of the computed density of states (DOS) and the crystal orbital Hamilton populations (COHP) are shown in Figure 6 and 7, respectively.

The first notable features of the DOS plots are the band gaps at the Fermi level, with sizes of 1.4 eV for $Ba_3Ga_3P_5$, 1.9 eV for $Ba_3Al_3P_5$, and 1.6 eV for $Ba_3Al_3As_5$, respectively. This suggests that the title compounds should be intrinsic semiconductors, as expected for Zintl compounds. These band gap values also correlate well with the colors of the crystals—$Ba_3Al_3P_5$ shows bright red color, and $Ba_3Ga_3P_5$ and $Ba_3Al_3As_5$ are dark-red when cut into very thin slices.

Examining the DOS curves reveals that the P or As p states and the Ba d states dominate the upper part of the valence and the lower part of the conduction bands, respectively. The states further below are predominately from the s, p orbitals from triel and pnictogen, with the s states lying below the p states. From the partial DOS of the triel and pnictogen atoms, it is evident that these states mix significantly, suggesting strong covalent

dx.doi.org/10.1021/ic302437t | *Inorg. Chem.* 2013, 52, 499−505

interactions. Mixing of the Ba d and the pnictogens p states is also observed, especially in the energy window just below the Fermi level from −2 to 0 eV, suggesting that Ba and pnictogen atoms play an important role in determining the transport property. Similar features in the electronic structures are noted for the thermoelectric materials Ca_3AlSb_3[28] and $Ca_5Al_2Sb_6$.[29]

The COHP diagrams of the selected atomic interactions are plotted in Figure 7. As seen from the figure, the *Tr*−*Pn* interactions show high COHP (i.e., very strong bonding), and they are fully optimized at the Fermi level. On the other hand, the Ba−*Pn* interactions are much weaker as judged by their COHP, and their bonding character is retained at the conduction band edge. However, they are unlikely to be optimized by *n*-doping since filling the states above the Fermi level will lead to the simultaneous occupation of the strongly antibonding *Tr*−*Pn* states, thus resulting in the destabilization of the overall structure. In this sense, the title compounds are expected to be p-type semiconductors in parallel with $Ca_5Tr_2Sb_6$ (*Tr* = Al, Ga, In),[55] where the formation of *n*-type material remains a challenge since strong Sb−Sb antibonding states of these compounds are lying just above the Fermi level.

CONCLUSION

$Ba_3Ga_3P_5$, $Ba_3Al_3P_5$, and $Ba_3Al_3As_5$ have been synthesized from flux reactions. They are isoelectronic and isostructual, crystallizing with a new rhombohedral structure in the space group $R\bar{3}c$. In the structure, $TrPn_4$ tetrahedra are formed and further condensed by sharing common corners and edges into a unique 3D framework; and Ba cations are occupying the octahedral holes created by *Pn* atoms. Computations on their electronic structures reveal band gaps for all three compounds, suggesting them to be semiconductors. Since they are similar to Ca_3AlSb_3 and $Ca_5Al_2Sb_6$, the charge- and heat-transport data could be of interest to the field of thermoelectrics, but their air-sensitivity hindered all measurements of their physical properties. The discovery of the title compounds has again proven the rich "phase-space" in these systems, which is worth further exploration.

ASSOCIATED CONTENT

Supporting Information

A combined X-ray crystallographic file in CIF format, and figures showing the computed band structures of the title compounds (LMTO method). This material is available free of charge via the Internet at http://pubs.acs.org.

AUTHOR INFORMATION

Corresponding Author

*Phone: (302) 831-8720. Fax: (302) 831-6335. E-mail: bobev@udel.edu.

Notes

The authors declare no competing financial interest.

ACKNOWLEDGMENTS

The authors gratefully acknowledge the financial support from the University of Delaware and U.S. Department of Energy through Grants DE-SC0001360 and DE-SC0008885.

REFERENCES

(1) Xia, S.-Q.; Hullmann, J.; Bobev, S.; Ozbay, A.; Nowak, E. R.; Fritsch, V. *J. Solid State Chem.* **2007**, *180*, 2088−2094.
(2) Hullmann, J.; Xia, S.-Q.; Bobev, S. *Acta Crystallogr.* **2007**, *E63*, i178.
(3) Xia, S. Q.; Hullmann, J.; Bobev, S. *J. Solid State Chem.* **2008**, *181*, 1909−1914.
(4) Bobev, S.; Hullmann, J.; Harmening, T.; Pöttgen, R. *Dalton Trans.* **2010**, *39*, 6049−6055.
(5) He, H.; Stearrett, R.; Nowak, E. R.; Bobev, S. *Inorg. Chem.* **2010**, *49*, 7935−7940.
(6) He, H.; Stearrett, R.; Nowak, E. R.; Bobev, S. *Eur. J. Inorg. Chem.* **2011**, 4025−4036.
(7) He, H.; Tyson, C.; Saito, M.; Bobev, S. *J. Solid State Chem.* **2012**, *188*, 59−65.
(8) (a) Cordier, G.; Schäfer, H. *Angew. Chem.* **1981**, *93*, 474−474. (b) Cordier, G.; Czech, E.; Jakowski, M.; Schäfer, H. *Rev. Chim. Miner.* **1981**, *18*, 9−18. (c) Cordier, G.; Schäfer, H.; Stelter, M. *Z. Naturforsch.* **1984**, *39*, 727−732. (d) Cordier, G.; Schäfer, H.; Stelter, M. *Z. Anorg. Allg. Chem.* **1984**, *519*, 183−188. (e) Cordier, G.; Stelter, M.; Schäfer, H. *J. Less-Common Metals* **1984**, *98*, 285−290. (f) Cordier, G.; Schäfer, H.; Stelter, M. *Z. Anorg. Allg. Chem.* **1985**, *40*, 1100−1104. (g) Cordier, G.; Schäfer, H.; Stelter, M. *Z. Naturforsch.* **1985**, *40*, 5−8.
(9) Kim, S. J.; Kanatzidis, M. G. *Inorg. Chem.* **2001**, *40*, 3781−3785.
(10) Todorov, I.; Chung, D. Y.; Ye, L.; Freeman, A. J.; Kanatzidis, M. G. *Inorg. Chem.* **2009**, *48*, 4768−4776.
(11) Mathieu, J.; Achey, R.; Park, J. H.; Purcell, K. M.; Tozer, S. W.; Latturner, S. E. *Chem. Mater.* **2008**, *20*, 5675−5681.
(12) Jiang, J.; Payne, A. C.; Olmstead, M. M.; Lee, H. O.; Klavins, P.; Fisk, Z.; Kauzlarich, S. M.; Hermann, R. P.; Grandjean, F.; Long, G. J. *Inorg. Chem.* **2005**, *44*, 2189−2197.
(13) Jiang, J.; Olmstead, M. M.; Kauzlarich, S. M.; Lee, H. O.; Klavins, P.; Fisk, Z. *Inorg. Chem.* **2005**, *44*, 5322−5327.
(14) Jiang, J.; Kauzlarich, S. M. *Chem. Mater.* **2006**, *18*, 435−441.
(15) Goforth, A. M.; Hope, H.; Condron, C. L.; Kauzlarich, S. M.; Jensen, N.; Klavins, P.; MaQuilon, S.; Fisk, Z. *Chem. Mater.* **2009**, *21*, 4480−4489.
(16) Park, S. M.; Kim, S. J.; Kanatzidis, M. G. *J. Solid State Chem.* **2003**, *175*, 310−315.
(17) Park, S. M.; Kim, S. J.; Kanatzidis, M. G. *J. Solid State Chem.* **2004**, *177*, 2867−2874.
(18) Schäfer, H.; Eisenmann, B.; Müller, W. *Angew. Chem., Int. Ed. Engl.* **1973**, *12*, 694−712.
(19) Nesper, R. *Prog. Solid State Chem.* **1990**, *20*, 1−45.
(20) Kauzlarich, S. M., Ed.; *Chemistry, Structure, and Bonding of Zintl Phases and Ions*; VCH Publishers: New York, 1996.
(21) Kauzlarich, S. M.; Brown, S. R.; Snyder, G. J. *Dalton Trans.* **2007**, 2099−2107.
(22) Toberer, E. S.; May, A. F.; Snyder, G. J. *Chem. Mater.* **2010**, *22*, 624−634.
(23) Snyder, G. J.; Toberer, E. S. *Nat. Mater.* **2008**, *7*, 105−114.
(24) Brown, S. R.; Kauzlarich, S. M.; Gascoin, F.; Snyder, G. J. *Chem. Mater.* **2006**, *18*, 1873−1877.
(25) Gascoin, F.; Ottensmann, S.; Stark, D.; Haïle, S. M.; Snyder, G. J. *Adv. Funct. Mater.* **2005**, *15*, 1860−1864.
(26) Zhang, H.; Zhao, J.-T.; Grin, Y.; Wang, X.-J.; Tang, M.-B.; Man, Z.-Y.; Chen, H.-H.; Yang, X.-X. *J. Chem. Phys.* **2008**, *129*, 164713.
(27) Zhang, H.; Baitinger, M.; Tang, M.-B.; Man, Z.-Y.; Chen, H.-H.; Yang, X.-X.; Liu, Y.; Chen, L.; Grin, Y.; Zhao, J.-T. *Dalton Trans.* **2010**, *39*, 1101−1104.
(28) Zevalkink, A.; Toberer, E. S.; Zeier, W. G.; Flage-Larsen, E.; Snyder, G. J. *Energy Environ. Sci.* **2011**, *4*, 510−518.
(29) Toberer, E. S.; Zevalkink, A.; Crisosto, N.; Snyder, J. G. *Adv. Funct. Mater.* **2010**, *20*, 4375−4380.
(30) Kanatzidis, M. G.; Pöttgen, R.; Jeitschko, W. *Angew. Chem., Int. Ed.* **2005**, *44*, 6996−7023.
(31) He, H.; Bobev, S. unpublished results: $Ba_7Ga_4As_9$ (*Pmmn*, *a* = 10.184(2) Å, *b* = 16.987(4) Å, *c* = 6.8012(14) Å) and $Ba_7Ga_4P_9$ (*Pmmn*, *a* = 9.877(2) Å, *b* = 16.548(4) Å, *c* = 6.6395(15) Å), both with $Ba_7Ga_4Sb_9$ structure type.
(32) Kauzlarich, S. M.; Thomas, M. M.; Odink, D. A.; Olmstead, M. M. *J. Am. Chem. Soc.* **1991**, *113*, 7205−7208.

(33) Villars, P.; Calvert, L. D., Eds.; *Pearson's Handbook of Crystallographic Data for Intermetallic Phases*, 2nd ed.; American Society for Metals: Materials Park, OH, 1991.
(34) *SMART NT*, Version 5.63; Bruker Analytical X-ray Systems, Inc.: Madison, WI, 2003.
(35) *SAINT NT*, Version 6.45; Bruker Analytical X-ray Systems, Inc.: Madison, WI, 2003.
(36) Sheldrick, G. M. *SADABS*; University of Göttingen: Göttingen, Germany, 2003.
(37) Sheldrick, G. M. *SHELXTL*; University of Göttingen: Göttingen, Germany, 2001.
(38) (a) Parthe, E.; Gelato, L. M. *Acta Crystallogr.* **1984**, *A40*, 169−183. (b) Gelato, L. M.; Parthe, E. *J. Appl. Crystallogr.* **1987**, *20*, 139−143.
(39) Jepsen, O.; Andersen, O. K. *TB-LMTO-ASAP program*, version 4.7; Max-Planck-Institut für Festkörperforschung: Stuttgart, Germany, 1998.
(40) Andersen, O. K.; Jepsen, O. *Phys. Rev. Lett.* **1984**, *53*, 2571−2574.
(41) Koelling, D. D.; Harmon, B. N. *J. Phys. C: Solid State Phys.* **1977**, *10*, 3107−3114.
(42) Blöchl, P. E.; Jepsen, O.; Andersen, O. K. *Phys. Rev. B* **1994**, *49*, 16223−16233.
(43) Dronskowski, R.; Blöchl, P. *J. Phys. Chem.* **1993**, *97*, 8617−8624.
(44) *ICSD Database*; FIZ, Fachinformationszentrum: Karlsruhe, Germany.
(45) Cordier, G.; Ochmann, H.; Schäfer, H. *Rev. Chim. Miner* **1984**, *21*, 282−291.
(46) Cordier, G.; Ochmann, H.; Schäfer, H. *Rev. Chim. Miner* **1985**, *22*, 58−63.
(47) Cordier, G.; Ochmann, H. *Z. Kristallogr.* **1991**, *197*, 295−296.
(48) Birdwhistell, T. L. T.; Stevens, E. D.; O'Connor, C. J. *Inorg. Chem.* **1990**, *29*, 3892−3894.
(49) Bobev, S.; Sevov, S. C. *J. Solid State Chem.* **2001**, *163*, 436−448.
(50) Clarke, S. J.; DiSalvo, F. J. *Inorg. Chem.* **1997**, *36*, 1143−1148.
(51) Hintze, F.; Hummel, F.; Schmidt, P. J.; Wiechert, D.; Schnick, W. *Chem. Mater.* **2012**, *24*, 402−407.
(52) Pauling, L. *The Nature of the Chemical Bond*, 3rd ed.; Cornell University Press: Ithaca, NY, 1960.
(53) Peters, K.; Carrillo-Cabrera, W.; Somer, M.; von Schnering, H.-G. *Z. Kristallogr.* **1996**, *211*, 53−53.
(54) (a) Shannon, R. D.; Prewitt, C. T. *Acta Crystallogr.* **1969**, *B25*, 925−945. (b) Shannon, R. D. *Acta Crystallogr.* **1976**, *A32*, 751−767.
(55) Zevalkink, A.; Pomrehn, G. S.; Johnson, S.; Swallow, J.; Gibbs, Z. M.; Snyder, G. J. *Chem. Mater.* **2012**, *24*, 2091−2098.